Benchmark study of symmetry-adapted ML-DFT models for magnetically doped topological insulators

March 27, 2023 | **Johannes Wasmer**[1] Rubel Mozumder[1] Philipp Rüßmann[2,1] Ira Assent[3,1] Stefan Blügel[1] | [1]Forschungszentrum Jülich [2]University of Würzburg [3]Aarhus University, Denmark

JÜLICH Forschungszentrum

Outline

Introduction

Database generation

ML experiments

Conclusion

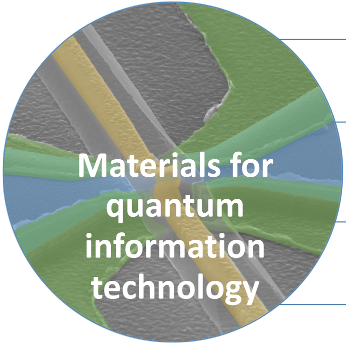

High-performance and high-throughput calculations

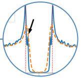

Superconductivity

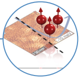

Ab initio impurity embedding

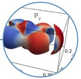

First principles electronic structure calculations

juDFT

AiiDA

Fleur

spirit

JuKKR

SPEX

Hands-on Tutorial
May 8-12, Jülich
flapw.de

Workshop
Sep 4-7, Athens
psi-k.net/workshops

Topological insulators and magnetic impurities

- Magnetic doping of topological insulators can induce a topological phase transition
  - Ferromagnetic ordering
  - Out-of-plane anisotropy

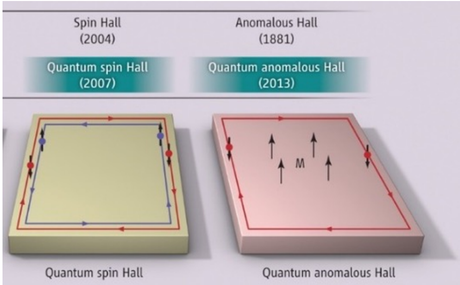

S. Oh, Science **340**, 153 (2013)

→ Topological insulator

Two counter propagating edge states

One single edge states

M || $\hat{z}$

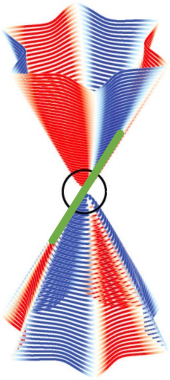

Henk *et al.*, PRL **109**, 076801 (2012)

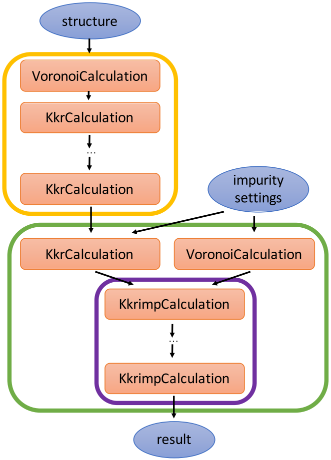

[a]

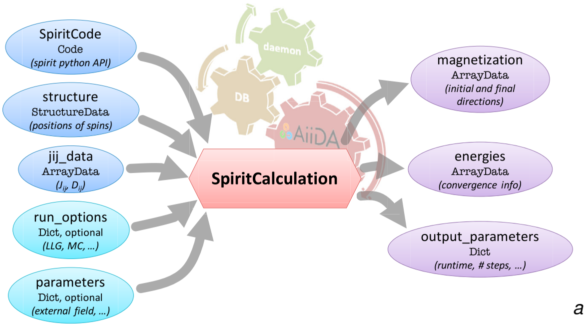

[a]

$$\mathcal{H} \approx -\sum_{\langle ij \rangle} J_{ij}\, \vec{S}_i \cdot \vec{S}_j - \sum_{\langle ij \rangle} \vec{D}_{ij} \cdot (\vec{S}_i \times \vec{S}_j)$$

$$\mathcal{J}_{ij} = -\frac{1}{\pi} \operatorname{Im} \int_{-\infty}^{E_F} \mathrm{d}E \, \mathrm{Tr}[\delta t_i G_{ij} \delta t_j G_{ji}]$$

$$\frac{\partial \mathbf{n}_i}{\partial t} = -\gamma' \mathbf{n}_i \times \mathbf{B}_i^{\text{eff}} - \lambda \mathbf{n}_i \times \left(\mathbf{n}_i \times \mathbf{B}_i^{\text{eff}} \right)$$

[a] Rüßmann, Bertoldo, and Blügel 2021.

[a] Rüßmann, Ribas Sobreviela, et al. 2022.

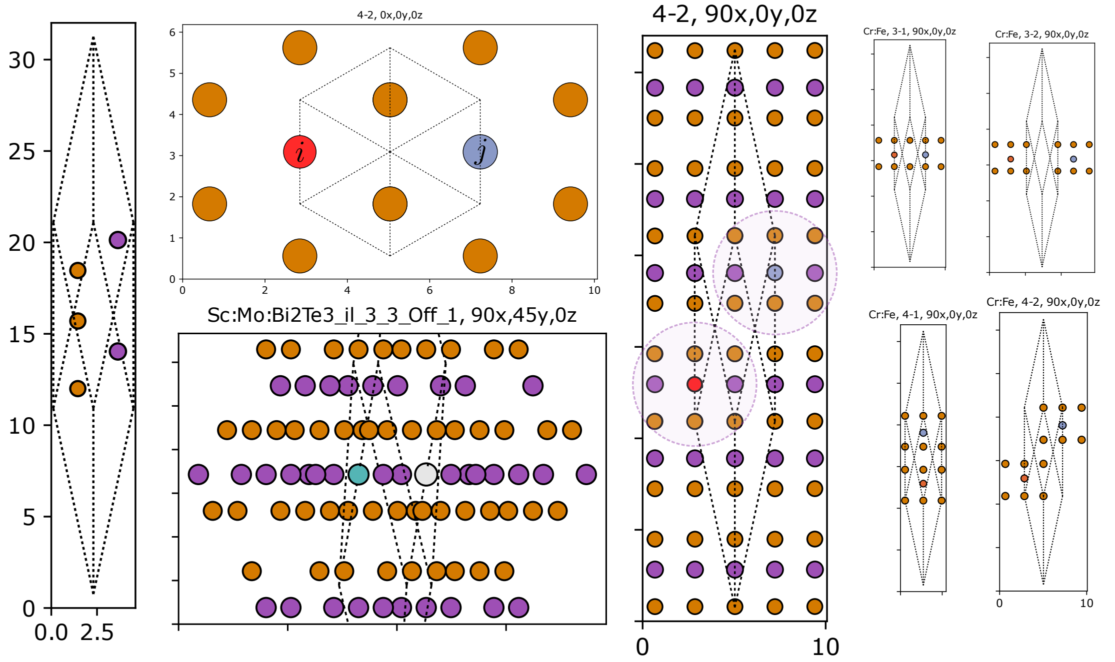

4-2, 0x,0y,0z
i
j
Sc:Mo:Bi2Te3_il_3_3_Off_1, 90x,45y,0z
4-2, 90x,0y,0z
Cr:Fe, 3-1, 90x,0y,0z
Cr:Fe, 3-2, 90x,0y,0z
Cr:Fe, 4-1, 90x,0y,0z
Cr:Fe, 4-2, 90x,0y,0z

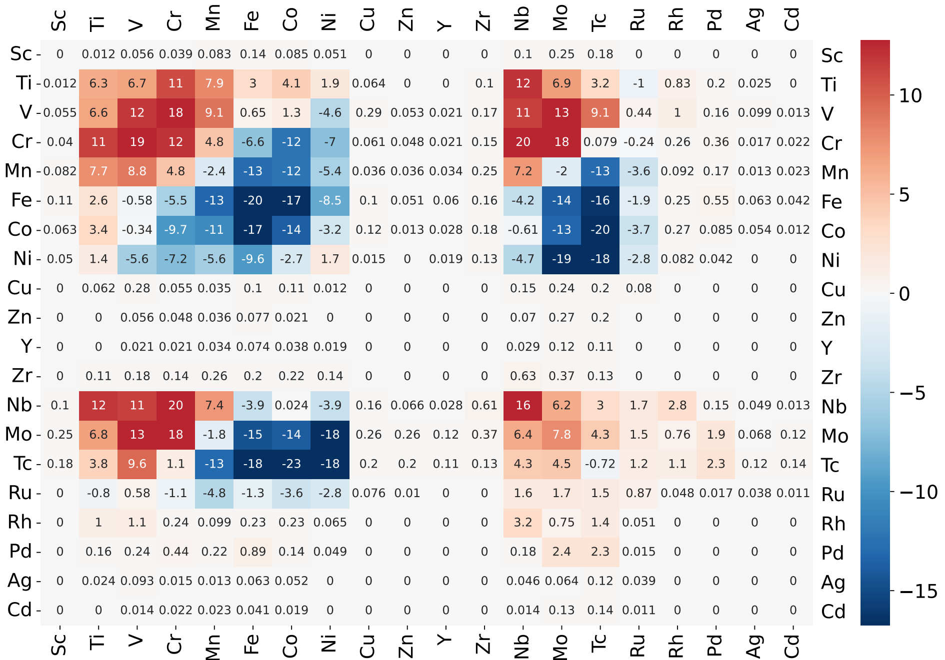
Sc Ti V Cr Mn Fe Co Ni Cu Zn Y Zr Nb Mo Tc Ru Rh Pd Ag Cd
Sc 0 0.012 0.056 0.039 0.083 0.14 0.085 0.051 0 0 0 0 0.1 0.25 0.18 0 0 0 0 0
Ti 0.012 6.3 6.7 11 7.9 3 4.1 1.9 0.064 0 0 0.1 12 6.9 3.2 -1 0.83 0.2 0.025 0
V 0.055 6.6 12 18 9.1 0.65 1.3 -4.6 0.29 0.053 0.021 0.17 11 13 9.1 0.44 1 0.16 0.099 0.013
Cr 0.04 11 19 12 4.8 -6.6 -12 -7 0.061 0.048 0.021 0.15 20 18 0.079 -0.24 0.26 0.36 0.017 0.022
Mn 0.082 7.7 8.8 4.8 -2.4 -13 -12 -5.4 0.036 0.036 0.034 0.25 7.2 -2 -13 -3.6 0.092 0.17 0.013 0.023
Fe 0.11 2.6 -0.58 -5.5 -13 -20 -17 -8.5 0.1 0.051 0.06 0.16 -4.2 -14 -16 -1.9 0.25 0.55 0.063 0.042
Co 0.063 3.4 -0.34 -9.7 -11 -17 -14 -3.2 0.12 0.013 0.028 0.18 -0.61 -13 -20 -3.7 0.27 0.085 0.054 0.012
Ni 0.05 1.4 -5.6 -7.2 -5.6 -9.6 -2.7 1.7 0.015 0 0.019 0.13 -4.7 -19 -18 -2.8 0.082 0.042 0 0
Cu 0 0.062 0.28 0.055 0.035 0.1 0.11 0.012 0 0 0 0 0.15 0.24 0.2 0.08 0 0 0 0
Zn 0 0 0.056 0.048 0.036 0.077 0.021 0 0 0 0 0 0.07 0.27 0.2 0 0 0 0 0
Y 0 0 0.021 0.021 0.034 0.074 0.038 0.019 0 0 0 0 0.029 0.12 0.11 0 0 0 0 0
Zr 0 0.11 0.18 0.14 0.26 0.2 0.22 0.14 0 0 0 0 0.63 0.37 0.13 0 0 0 0 0
Nb 0.1 12 11 20 7.4 -3.9 0.024 -3.9 0.16 0.066 0.028 0.61 16 6.2 3 1.7 2.8 0.15 0.049 0.013
Mo 0.25 6.8 13 18 -1.8 -15 -14 -18 0.26 0.26 0.12 0.37 6.4 7.8 4.3 1.5 0.76 1.9 0.068 0.12
Tc 0.18 3.8 9.6 1.1 -13 -18 -23 -18 0.2 0.2 0.11 0.13 4.3 4.5 -0.72 1.2 1.1 2.3 0.12 0.14
Ru 0 -0.8 0.58 -1.1 -4.8 -1.3 -3.6 -2.8 0.076 0.01 0 0 1.6 1.7 1.5 0.87 0.048 0.017 0.038 0.011
Rh 0 1 1.1 0.24 0.099 0.23 0.23 0.065 0 0 0 0 3.2 0.75 1.4 0.051 0 0 0 0
Pd 0 0.16 0.24 0.44 0.22 0.89 0.14 0.049 0 0 0 0 0.18 2.4 2.3 0.015 0 0 0 0
Ag 0 0.024 0.093 0.015 0.013 0.063 0.052 0 0 0 0 0 0.046 0.064 0.12 0.039 0 0 0 0
Cd 0 0 0.014 0.022 0.023 0.041 0.019 0 0 0 0 0 0.014 0.13 0.14 0.011 0 0 0 0
10
5
0
−5
−10
−15

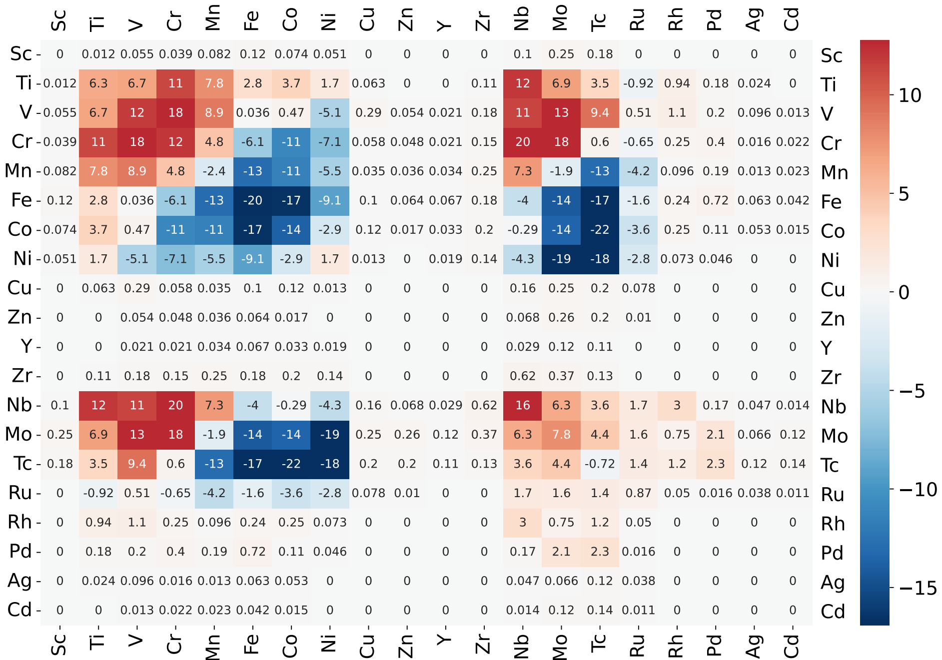
Sc Ti V Cr Mn Fe Co Ni Cu Zn Y Zr Nb Mo Tc Ru Rh Pd Ag Cd
Sc 0 0.012 0.055 0.039 0.082 0.12 0.074 0.051 0 0 0 0 0.1 0.25 0.18 0 0 0 0 0
Ti 0.012 6.3 6.7 11 7.8 2.8 3.7 1.7 0.063 0 0 0.11 12 6.9 3.5 -0.92 0.94 0.18 0.024 0
V 0.055 6.7 12 18 8.9 0.036 0.47 -5.1 0.29 0.054 0.021 0.18 11 13 9.4 0.51 1.1 0.2 0.096 0.013
Cr 0.039 11 18 12 4.8 -6.1 -11 -7.1 0.058 0.048 0.021 0.15 20 18 0.6 -0.65 0.25 0.4 0.016 0.022
Mn 0.082 7.8 8.9 4.8 -2.4 -13 -11 -5.5 0.035 0.036 0.034 0.25 7.3 -1.9 -13 -4.2 0.096 0.19 0.013 0.023
Fe 0.12 2.8 0.036 -6.1 -13 -20 -17 -9.1 0.1 0.064 0.067 0.18 -4 -14 -17 -1.6 0.24 0.72 0.063 0.042
Co 0.074 3.7 0.47 -11 -11 -17 -14 -2.9 0.12 0.017 0.033 0.2 -0.29 -14 -22 -3.6 0.25 0.11 0.053 0.015
Ni 0.051 1.7 -5.1 -7.1 -5.5 -9.1 -2.9 1.7 0.013 0 0.019 0.14 -4.3 -19 -18 -2.8 0.073 0.046 0 0
Cu 0 0.063 0.29 0.058 0.035 0.1 0.12 0.013 0 0 0 0 0.16 0.25 0.2 0.078 0 0 0 0
Zn 0 0 0.054 0.048 0.036 0.064 0.017 0 0 0 0 0 0.068 0.26 0.2 0.01 0 0 0 0
Y 0 0 0.021 0.021 0.034 0.067 0.033 0.019 0 0 0 0 0.029 0.12 0.11 0 0 0 0 0
Zr 0 0.11 0.18 0.15 0.25 0.18 0.2 0.14 0 0 0 0 0.62 0.37 0.13 0 0 0 0 0
Nb 0.1 12 11 20 7.3 -4 -0.29 -4.3 0.16 0.068 0.029 0.62 16 6.3 3.6 1.7 3 0.17 0.047 0.014
Mo 0.25 6.9 13 18 -1.9 -14 -14 -19 0.25 0.26 0.12 0.37 6.3 7.8 4.4 1.6 0.75 2.1 0.066 0.12
Tc 0.18 3.5 9.4 0.6 -13 -17 -22 -18 0.2 0.2 0.11 0.13 3.6 4.4 -0.72 1.4 1.2 2.3 0.12 0.14
Ru 0 -0.92 0.51 -0.65 -4.2 -1.6 -3.6 -2.8 0.078 0.01 0 0 1.7 1.6 1.4 0.87 0.05 0.016 0.038 0.011
Rh 0 0.94 1.1 0.25 0.096 0.24 0.25 0.073 0 0 0 0 3 0.75 1.2 0.05 0 0 0 0
Pd 0 0.18 0.2 0.4 0.19 0.72 0.11 0.046 0 0 0 0 0.17 2.1 2.3 0.016 0 0 0 0
Ag 0 0.024 0.096 0.016 0.013 0.063 0.053 0 0 0 0 0 0.047 0.066 0.12 0.038 0 0 0 0
Cd 0 0 0.013 0.022 0.023 0.042 0.015 0 0 0 0 0 0.014 0.12 0.14 0.011 0 0 0 0
10
5
0
−5
−10
−15

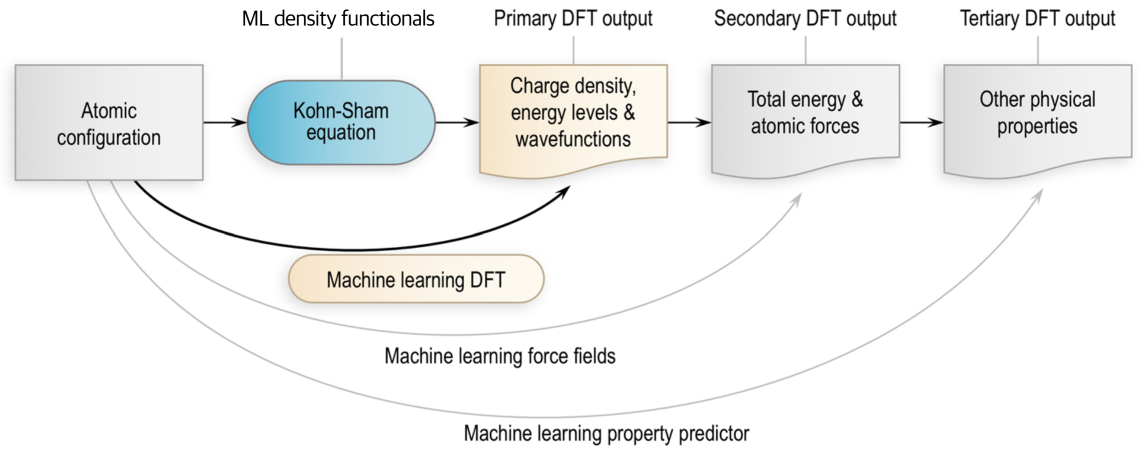

[1]

[1] Chandrasekaran et al. 2019.

Descriptors: Coulomb Matrix, SOAP.

Models: Kernel ridge regression.
Kernels: Linear, Gauss, Laplace.

$$M_{ij}^{\text{Coulomb}} = \begin{cases} 0.5 Z_i^2 \\ \frac{Z_i Z_j}{R_{ij}} \end{cases}$$

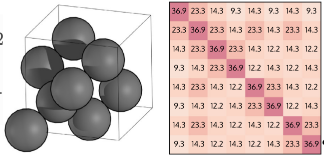

36.9	23.3	14.3	9.3	14.3	9.3	14.3	9.3
23.3	36.9	23.3	14.3	23.3	14.3	23.3	14.3
14.3	23.3	36.9	23.3	14.3	12.2	14.3	12.2
9.3	14.3	23.3	36.9	12.2	14.3	12.2	14.3
14.3	23.3	14.3	12.2	36.9	23.3	14.3	12.2
9.3	14.3	12.2	14.3	23.3	36.9	12.2	14.3
14.3	23.3	14.3	12.2	14.3	12.2	36.9	23.3
9.3	14.3	12.2	14.3	12.2	14.3	23.3	36.9

[a]

$$\hat{y}(A) = \sum_{i}^{N} c_i \, \kappa \left(\phi(A), \phi(A^{(i)}) \right)$$

$$\mathbf{c} = (\mathbf{K} + \alpha \, \mathbf{I}_m)^{-1} \, \mathbf{y}$$

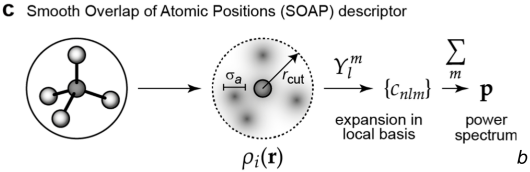

[b]

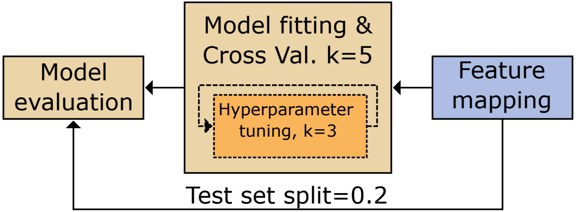

[a]Himanen et al. 2020.
[b]Deringer et al. 2021.

Results

Average model performance in 5x3 CV[1], N = 1728 samples.

Model	$\overline{t_{train}}$	$\overline{t_{test}}$	$\overline{\mathrm{MAE}}$	$\overline{\mathrm{R}^2}$
CM-KKR-lin-rcut-4.0	1.44	0.01	1.56	-2.14
CM-KRR-lap-rcut-4.0	2.54	0.04	**0.50**	**0.54**
CM-KRR-lap-rcut-7.6	54.1	2.12	0.53	0.53
SOAP-KRR-lin-rcut-4.0	52.6	0.83	0.87	0.01
SOAP-KRR-rbf-rcut-4.0	160	0.90	**0.46**	**0.73**

Best model from 5x3 CV, performance on test set.

Model	MAE	R^2
CM-KKR-lin-rcut-4.0	1.15	-0.01
CM-KRR-lap-rcut-4.0	**0.05**	**0.99**
CM-KRR-lap-rcut-7.6	0.05	0.99
SOAP-KRR-lin-rcut-4.0	0.87	0.01
SOAP-KRR-rbf-rcut-4.0	**0.12**	**0.96**

[1] MAE unit is meV, time is seconds. Hyperparameter grid sizes $\sim$3x3.

Results

Parity plots

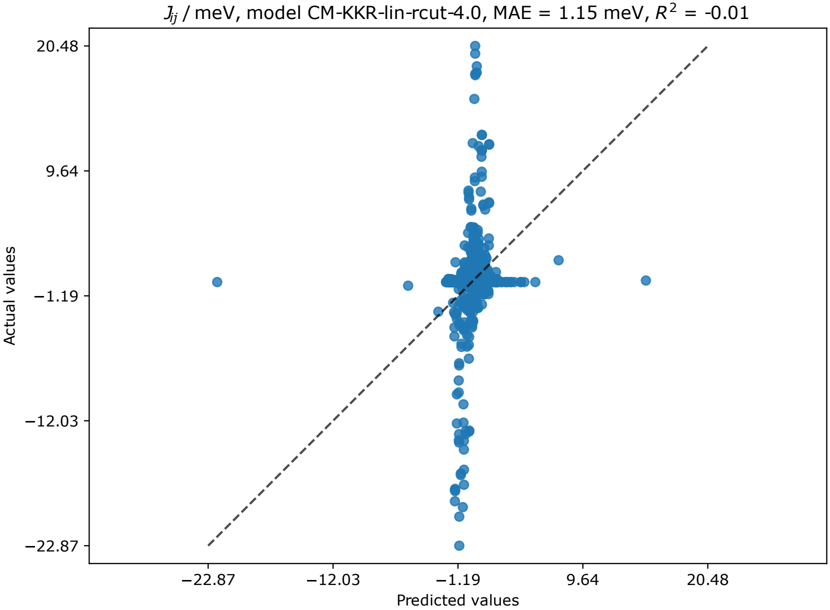

Results

Parity plots

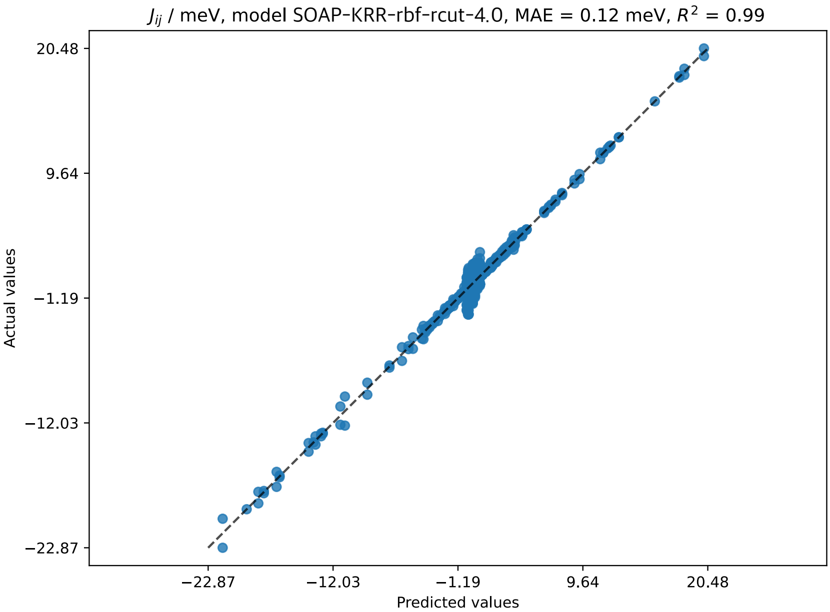

Conclusion

- Benchmarked symmetry-adapated ML surrogate models for exchange coupling constant J_{ij} for magnetically co-doped TI Bi_2Te_3
- Only non-linear kernels manage to capture the structure-property relationship
- CM showed better test performance, SOAP better average performance despite large chemical space (22 elements)
- Larger atomic environment did not improve performance (CM; SOAP not tested)
- Extend from 2 to N defect atoms
- Evaluate advanced models (sparser[1], higher body-order[2])

[1] Lopanitsyna et al. 2022.
[2] Batatia et al. 2022.

Workshop

4-7.09.2023 in Athens, Greece

First-principles Green function formalisms: algorithms, method developments and applications to spinorbitronics and magneto-superconductivity

https://go.fzj.de/gf2023

Recommended talks

- Mon, 15:30, TT 3.2. Yu-Shiba-Rusinov impurity bound states in superconductors from first principles. David Antognini Silva.
- Fri, 12:15, TT 63.11. Ab initio study of magnetic doping in an Ising superconductor. Mohammad Hemmati.

References I

- Batatia, Ilyes et al. (June 15, 2022). MACE: Higher Order Equivariant Message Passing Neural Networks for Fast and Accurate Force Fields. DOI: 10.48550/arXiv.2206.07697. arXiv: 2206.07697 [cond-mat, physics:physics, stat]. URL: http://arxiv.org/abs/2206.07697 (visited on 09/25/2022).
- Chandrasekaran, Anand et al. (Feb. 18, 2019). “Solving the Electronic Structure Problem with Machine Learning”. In: npj Computational Materials 5.1 (1), pp. 1–7. ISSN: 2057-3960. DOI: 10.1038/s41524-019-0162-7. URL: https://www.nature.com/articles/s41524-019-0162-7 (visited on 08/21/2021).
- Deringer, Volker L. et al. (Aug. 25, 2021). “Gaussian Process Regression for Materials and Molecules”. In: Chemical Reviews 121.16, pp. 10073–10141. ISSN: 0009-2665. DOI: 10.1021/acs.chemrev.1c00022. URL: https://doi.org/10.1021/acs.chemrev.1c00022 (visited on 06/03/2022).

References II

- Himanen, Lauri et al. (Feb. 1, 2020). “DScribe: Library of Descriptors for Machine Learning in Materials Science”. In: Computer Physics Communications 247, p. 106949. ISSN: 0010-4655. DOI: 10.1016/j.cpc.2019.106949. URL: https://www.sciencedirect.com/science/article/pii/S0010465519303042 (visited on 05/13/2021).
- Lopanitsyna, Nataliya et al. (Dec. 26, 2022). Modeling High-Entropy Transition-Metal Alloys with Alchemical Compression. DOI: 10.48550/arXiv.2212.13254. arXiv: 2212.13254 [cond-mat, physics:physics]. URL: http://arxiv.org/abs/2212.13254 (visited on 12/29/2022).
- Rüßmann, Philipp, Fabian Bertoldo, and Stefan Blügel (Jan. 26, 2021). “The AiiDA-KKR Plugin and Its Application to High-Throughput Impurity Embedding into a Topological Insulator”. In: npj Computational Materials 7.1 (1), pp. 1–9. ISSN: 2057-3960. DOI: 10.1038/s41524-020-00482-5. URL: https://www.nature.com/articles/s41524-020-00482-5 (visited on 05/13/2021).

References III

Rüßmann, Philipp, Jordi Ribas Sobreviela, et al. (2022). “The AiiDA-Spirit Plugin for Automated Spin-Dynamics Simulations and Multi-Scale Modeling Based on First-Principles Calculations”. In: Frontiers in Materials 9. ISSN: 2296-8016. DOI: 10.3389/fmats.2022.825043. URL: https://www.frontiersin.org/articles/10.3389/fmats.2022.825043 (visited on 08/11/2022).

Discussion slides